PERGAMON

Building and Environment 34 (1999) 293–303

BUILDING AND ENVIRONMENT

Parameter estimation of unknown air exchange rates and effective mixing volumes from tracer gas measurements for complex multi-zone indoor air models

Michael D. Sohn[a,*], Mitchell J. Small[a,b]

[a] *Departments of Civil and Environmental Engineering, Carnegie Mellon University, Pittsburgh, Pennsylvania 15213, U.S.A.*
[b] *Engineering and Public Policy, Carnegie Mellon University, Pittsburgh, Pennsylvania 15213, U.S.A.*

Received 6 December 1996; revised 26 February 1998; accepted 7 April 1998

Abstract

The steepest descent and simulated annealing optimization techniques are used to simultaneously estimate the effective mixing volumes and air exchange rates of a large partitionless building exhibiting heterogeneous spatial air flow conditions. The optimization is conducted using varying quantities and qualities of simulated tracer gas measurements. A simulated three-compartment system is numerically investigated to assess the performance of the parameter estimation methods. When simulated tracer gases are released in each zone, both techniques estimate actual parameter values within 10–35 percent. When tracers are released in selected zones, reasonable estimates were obtained for those zones in which a simulated gas was released, but significant errors are evident for the non-release zones.

Nomenclature

C_i concentration of contaminant or tracer gas in zone i
S_i mass release rate of contaminant or tracer gas in zone i
V_i volume of zone i
f_{ij} rate of air flow from zone i to zone j
n number of zones

1. Introduction

Interest in air flow patterns, distribution, infiltration and energy loss in residential and occupational buildings can be traced back to economic issues related to the energy crisis two decades ago [1, 2]. As the cost of heating, cooling and ventilating a building rose, buildings were designed and constructed to reduce the exchange of air and heat between a building and the outside. In recent years, concerns related to indoor air pollution, caused in part by 'tighter' buildings and in part by physical, chemical, or biological contaminants in building materials, furnishings, processes or the ventilation system itself, have increased the need for effective characterization of building ventilation. As a result, a number of studies on air flow and infiltration based on Sinden's first-order multi-compartmental conservation of mass approach [3] (illustrated in Fig. 1 and formulated as Equation 1) have been conducted.[1] This paper intends to expand the set of analytical tools available for conducting and interpreting such studies, by identifying optimization methods for simultaneously estimating effective compartmental volumes and air exchange rates.

$$V_i \frac{\partial C_i}{\partial t} = S_i - C_i \sum_{j=0}^{n} f_{ij} + \sum_{j=0}^{n} C_j f_{ji}: \quad \text{for } i = 1, n \tag{1}$$

1.1. Model calibration

The inter-zonal air exchange rates for Sinden's model can be calibrated using tracer studies; most commonly the constant source/injection method [4–6] or the decay method [4, 5]. In both methods, different inert tracer gases, not found in or near the building (so that $C_o = 0$ and S_i is controlled), are simultaneously released and measured in each of the building compartments. Hence, a building comprised of n compartments (not including the outside) requires n tracer gases.

*Corresponding author. Tel.: 001 412 268 2940; fax: 001 412 268 7813.

[1] Sinden's approach assumes constant volumes and air exchange rates. While this may be an over simplification in many systems, this model has been widely used for demonstration purposes and found to be appropriate for many indoor air quality assessments.

S0360-1323/99 $—see front matter
PII: S0360-1323(98)00022-5

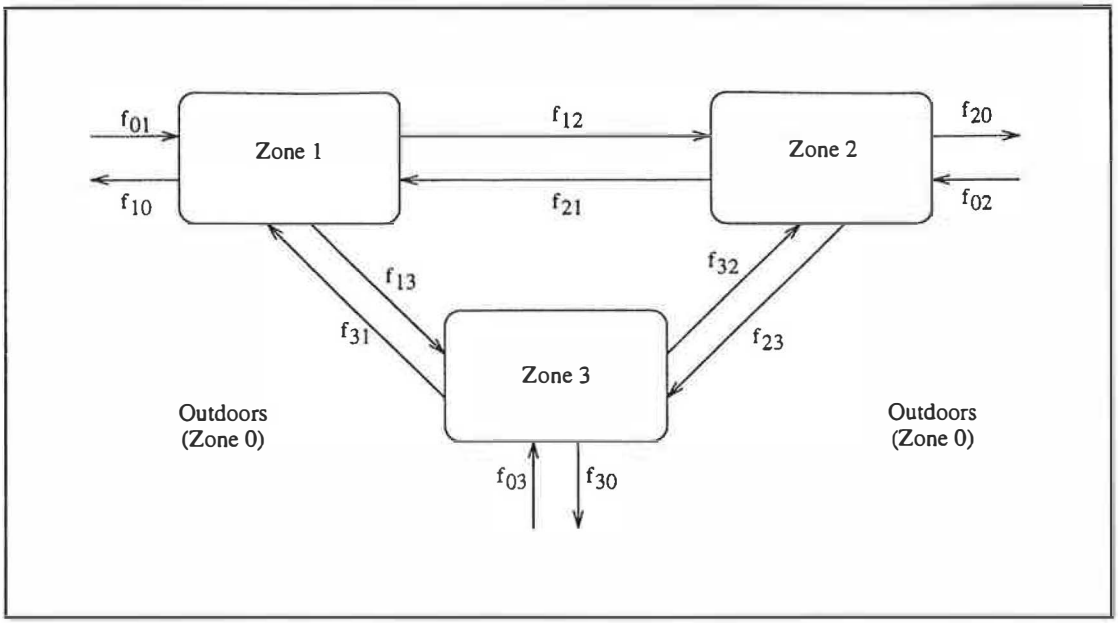

Fig. 1. Illustration of a three compartment plus 'outside' indoor air model.

In the constant source method, the tracer gases are released until steady-state gas concentrations are achieved in each compartment so that Equation 1 reduces to Equation 2.

$$0 = S_i - C_i \sum_{j=0}^{n} f_{ij} + \sum_{j=1}^{n} C_j f_{ji}: \quad \text{for } i = 1, n \tag{2}$$

The n^2+n unknown air exchange rates are estimated using the n sets of compartmental concentrations, one for each tracer gas released (yielding $n \times n = n^2$ measurements and corresponding equations), and the air flow conservation constraint for each compartment (yielding n equations):

$$\sum_{j=0}^{n} f_{ji} = \sum_{j=0}^{n} f_{ij}: \quad \text{for } i = 1, n \tag{3}$$

In the decay method, tracer gas is released as an initial pulse ($t \leqslant 0$) and the emission rate is zero thereafter ($t > 0$). Assuming that the duration of the pulse is short relative to the mixing rates, the release is assumed to occur instantaneously so that Equation 1 reduces to Equation 4.

$$V_i \frac{\partial C_i}{\partial t} = -C_i \sum_{j=0}^{n} f_{ij} + \sum_{j=1}^{n} C_j f_{ji}: \quad \text{for } i = 1, n \tag{4}$$

The n^2+n unknown air exchange rates are solved by simultaneously integrating the n^2 equations for the period of observation and invoking the n conservation of flow equations. The reader is referred to Lagus and Persily's study for a detailed description of the procedure [4].

1.2. Motivation

Central premises of both of the multi-zone calibration methods are that: (i) the number, location and size of each well-mixed zone are known a priori, and (ii) tracer gases can be successfully released in each zone. These assumptions are often appropriate for average size residential buildings, since intra-room mixing is usually orders of magnitude faster than inter-room air exchange and physical walls act as partitions for each zone, so that each room may act like a well-mixed compartment. However, in very large rooms with localized ventilation and/or source locations, a significant spatial concentration gradient may persist, dictating that the single well-mixed compartment approach may be inappropriate. Hence, the first-order approach must be abandoned for a more mechanistic second-order model (e.g., [7]). However, the latter approach can be computationally intensive and in some cases, sufficient data may not be available to estimate the parameters of the model for estimating building-wide ventilation or long-term human exposure.

We suggest that a large compartment may instead be satisfactorily represented as a combination of several well-mixed *surrogate zones* which are spatially located so as to capture the significant portions of the concentration gradient across the room. This maintains the simplicity of the well-mixed, first-order, conservation of mass approach, yet captures some of the heterogeneity in the room. Unfortunately, there is considerable difficulty in determining the appropriate number, location and size of the surrogate zones and the corresponding inter-zonal

air exchange rates. Qualitative experiments (e.g., visual smoke candle releases) can be used to help guide selection of the relative number and location of each surrogate zone within the room. Nevertheless, without exactly knowing the effective mixing volumes for each surrogate zone, neither of the two parameter estimation techniques discussed above can be used to estimate the effective inter-zonal air exchange rates.

An appropriate estimation technique must be able to simultaneously estimate the effective mixing volumes and the air exchange rates given the number of surrogate zones and their relative locations. The method should also be capable of making reasonable estimates when tracer gases have not been released in each of the zones, since, in many cases, there will be difficulty accurately releasing the gases in the partitionless area. To our knowledge, there is no analytical or numerical transformation that can be designed so that a system of equations can be directly solved for all possible unknown volumes and inter-compartmental air exchange rates in this case.

O'Neill and Crawford [8] suggest an approach using a least squares regression technique in which a single tracer gas is released in each compartment. They demonstrate their approach in a controlled experimental facility for a simplified three-zone model, where four of the twelve unknown flow rates were eliminated (set to zero) and three could then be solved using conservation of net flow; leaving only five air exchange rates and the three volumes to be estimated. In addition, tracer gas measurements obtained for the demonstration exhibited very little noise. The performance of the algorithm was not tested for cases where significant measurement error was present. Hence, the presence of local solutions to the least squares regression (directly influenced by the number of unknown air exchange rates, the noise in the measurements and the requirement that gases be released in each zone) has not yet been considered.

We evaluate a general approach using standard optimization techniques. The suggested optimization algorithms seek to minimize an objective function that allows for estimation of unknown compartmental volumes and flow rates, for cases in which tracer gases are not released in every zone. Two optimization techniques are considered. First, the relatively simple technique of steepest descent optimization is applied and shown to be effective in cases where a tracer gas is successfully released and measured in every zone. Second, the more complicated and computationally intensive technique of simulated annealing optimization is demonstrated as a possible solution method for the case in which an incomplete set of measurements results in local minimum solutions which render the steepest descent technique ineffective. Similar optimization techniques introduced in this paper have been successfully applied in other applications (e.g., [9, 10, 11]).

It is important to note that the purpose of this paper is not to identify the best or most efficient optimization algorithm possible for a specific application. Rather, we wish to promote further investigation of parameter optimization techniques for IAQ models by demonstrating the capabilities and limitations of two widely-used algorithms. Further study of this topic will allow for improved estimation efficiency and algorithm development.

2. Optimization for parameter estimation

Parameter estimation using combinatorial optimization is primarily used for problems where direct analytical or numerical estimates cannot be determined, or when it is computationally infeasible to do so. In other words, we know there is some combination of volumes and air exchange rates that will best describe the system of interest, but there is no direct method of finding it. In optimization, possible solution combinations are indirectly evaluated by comparing possible solutions to optimization criteria, commonly termed the objective function [10], which characterizes the fit of the predicted to the measured concentrations. The algorithm 'solves' the problem (i.e., estimates the parameters) when it minimizes (or maximizes, depending on how the criteria is described) the value of the objective function.

In this application, the minimization of the sum of the square difference between predicted and measured zonal concentrations (Σ(measured—predicted)^2: for all data) was chosen as the objective function. The minimum square error criteria is commonly used for its correspondence to mean value prediction in linear or non-linear regression and its ability to describe the overall trend in the model prediction without being overly influenced by outliers. Figure 2 illustrates the optimization routine. Upon initialization of the volumes and air exchange rates, the IAQ model is evaluated and concentrations are predicted. Optimality is then evaluated and if necessary, new parameter values are chosen based on the optimization method's search algorithm. With each iteration, the solution vector is checked to ensure that physical constraints are not violated before concentrations are again predicted. The procedures and properties of the steepest descent and simulated annealing methods are briefly discussed, followed by an illustrative application.

2.1. Steepest descent

Steepest descent is a simple and robust method for optimization when the solution field contains only one possible minimum (or maximum) solution vector. The algorithm has no method of differentiating between the global optimum and a local convergent solution. Estimation is achieved by iteratively *traveling* in the direction that yields the greatest improvement of the objective

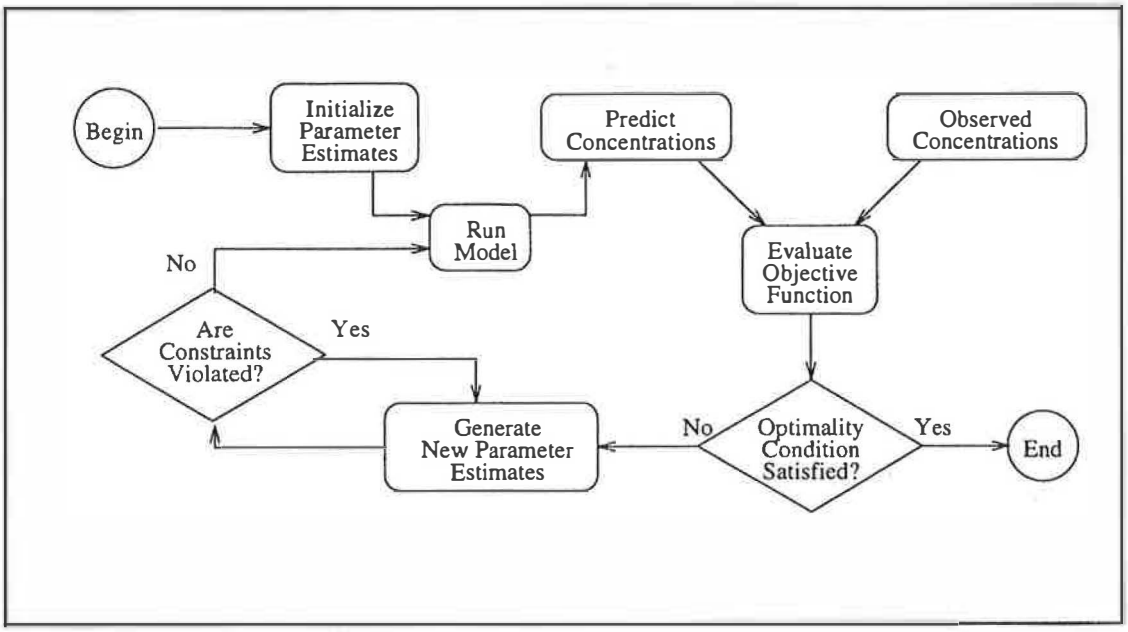

Fig. 2. Illustrative description of the optimization algorithm for parameter estimation (adapted from Fig. 3 in [10]).

function. Commonly, this is conducted by first evaluating the gradient of the objective function as a function of each decision variable (i.e., unknown parameter). The perturbation with the steepest slope is selected as the next iteration, and is continually updated until the gradient changes sign (i.e., the objective function cannot be further improved moving along this path). At this point, all of the parameter gradients are re-evaluated and updating is conducted again following the parameter yielding the steepest slope.

2.2. *Simulated annealing*

In cases where the solution field contains many locally optimal solutions, any parameter estimation algorithm will have difficulty differentiating between the globally and locally optimal combination(s). Aside from exhaustively evaluating all possible combinations, there is no computational method capable of providing a definite solution to such systems. Obtaining a 'very good' solution that is physically plausible (i.e., consistent with constraints) may be the most that can be expected.

The central principle of simulated annealing is the sporadic willingness of the algorithm to accept a worse parameter combination assuming that, by chance, the current solution is at, or on the road to, a local minimum combination [12, 13]. By accepting a worse combination when specific conditions are met, the algorithm allows itself the chance to 'jump' out of a local minimum and follow a different search path. The method is analogous to procedures used for metal refinement. To reduce a metal from a high to low energy state in which the atomic structure is arranged in a more orderly manner, the metal is first heated to a very high energy state and then cooled slowly following a strict temperature schedule. If the metal is cooled too quickly (i.e., quenched), the atomic structure may not have sufficient time to become properly arranged. As a result, the quenched metal may not achieve the desired low energy state. Similarly, if the parameter estimation algorithm quickly moves to the first minimum found in the solution field and stops, it is as if estimation was quenched and the resulting optimal combination will most likely be at a local minimum. Instead, the algorithm improves the chance of finding lower energy levels by slowly searching the full field of possible combinations, always accepting better combinations and allowing for the occasional parameter combination in a new domain of the parameter space that is less optimal than the current iteration.

At each iteration, the algorithm generates a possible combination of decision variables by changing the value of a random number of parameters in the previous combination. If the new combination does not violate any constraints, the IAQ model and the objective function are evaluated. If the value of the objective function is worse than the previous solution, a randomly generated value, uniformly distributed between 0 and 1, is compared to the value of P defined as Equation 5:

$$P = exp[-(E_2 - E_1)/kT] \tag{5}$$

where: E_1 and E_2 are the values of the objective function at the previous and current iterations, respectively; k is a scaling parameter and T is the dynamic annealing temperature.

Only when the random number is less than P is the worse combination accepted. If the value of the objective function is less than the previous solution, the combination is always accepted and the value of T is decremented. Note that as T decreases, the threshold probability, P, decreases, so that acceptance of less optimal solutions becomes less likely.

When the number of rejections at the current combination is greater than a specified amount (i.e., the algorithm cannot find a better combination or will not accept a worse combination because either the temperature is too low or the increase in energy to the suggested combinations is too great) the optimization is completed.

Notice that this method does not guarantee absolute convergence; termination is strictly dictated by the number of attempts made to move from the current combination. Irrespective of whether the lowest energy state has been found (i.e., the predicted volumes and air exchange rates are not the best fitting combination), the results may be close enough to the actual values for appropriate applications (e.g., building-wide ventilation and long-term IAQ studies).

Note also that the evaluation of the IAQ model requires the division of the air exchange rate by the effective mixing volume. It is therefore mathematically feasible to have a domain of parameter combinations that may equally match the best fitting parameter combination (i.e., there is an indeterminate solution). The possibility of this occurring increases as the number of zones where a tracer gas is released decreases. However, by using constraints to limit the search domain based on knowledge of the physical system, and by understanding the limits of the estimation techniques of these cases, it is likely that the occurrence of these circumstances can be limited or, if they do occur, be recognizable.

3. An illustrative demonstration

3.1. Description of the demonstration model

The three-zone model illustrated in Fig. 1 has been widely used as a demonstration system for applications in multi-zone modeling. Each zone is allowed to interact with the other compartments and the outside environment, which is assumed to act as a perfect sink with zero concentration and infinite volume. To evaluate the IAQ model, Equation 1 is numerically integrated using the 4th-order Runga-Kutta technique [14], chosen because of its robustness, stability and ease of computation. In addition, ill-conditioning of the matrix of air exchange rates does not contribute to numerical error of the solutions, since these solutions are not dependent on direct estimation of the determinate of the matrix as in the eigenvalue approach used by Sinden [3] (see also discussion in most elementary texts on differential equations, such as [15]).

To test the alternative parameter estimation methods, synthetic tracer gas concentrations were simulated by evaluating the IAQ model with separate unit releases of a tracer gas in each of the three zones. Table 1 (second column) summarizes the assumed parameter values for the test simulations. Noise was generated in the dataset by assuming a normally distributed measurement error structure with a standard deviation proportional to the true value[2] (i.e., a fixed coefficient of variation (COV)). Figure 3 depicts four experimental cases for a unit gas released in Zone 1 for a duration of 150 s, ranging from relatively precise (COV = 0.1) and frequent (every 50 s) measurements (Case A) to imprecise (COV = 0.5) and infrequent (every 150 s for 35 min and every 300 s thereafter) measurements (Case D). Similar synthetic measurements are simulated for a unit source release in Zone 2 and in Zone 3 under the same cases but, for brevity, are not illustrated here. Also, three levels of available data were considered for the release of different tracer gases: (i) in all three zones; (ii) in Zones 1 and 2; and (iii) only in Zone 1. The four cases and three conditions are thought to span the range of results that could typically be encountered in a tracer study of a building comprised of three partitionless surrogate zones.

3.2. Results and discussion

Initial values of the surrogate zones' volumes and air exchange rates were set close to zero. Constraints to the optimization routines included limiting the sum of the three compartment volumes to be less than or equal to an assumed total building volume (note that the effective mixing volume in the simulations was assumed to be 90% of the building volume), and non-negativity for both the volumes and air exchange rates. These minimal constraints were chosen, since little understanding is often available to make better initial guesses or place tighter constraints on the unknown parameters in the partitionless zones.

The standard steepest descent algorithm was unable to converge to an optimal solution because the search routine began to oscillate between selections as the algorithm approached the actual values. This occurred because the algorithm re-evaluates the gradients of the objective function only when the objective function cannot be improved by continuing to proceed along the current path. This results in parameters overshooting their optimal values far enough that when the gradients are re-evaluated, the

[2] When the measurement error generating procedure yielded a negative concentration, as can occur when assuming a normally distributed error structure, the value was replaced with a zero concentration. This parallels the assignment of a zero concentration to a measurement when an experiment yielded a de minimus concentration (i.e., below detection limit).

Table 1
Summary of the optimization results for the condition when a different tracer gas was released in each surrogate zone. The percent error from the actual values are in parentheses. C1, C2 and C3 are the steady-state concentrations for a unit release in Zone 1 for Zones 1, 2 and 3, respectively

		Steepest descent				Simulated annealing			
Case:	Actual	A	B	C	D	A	B	C	D
V1 (m3)	40	41 (3%)	45 (13%)	42 (5%)	49 (23%)	41 (3%)	45 (13%)	42 (5%)	45 (13%)
V2 (m3)	20	18 (10%)	13 (35%)	18 (10%)	13 (35%)	18 (10%)	13 (35%)	18 (10%)	13 (35%)
V3 (m3)	60	60 (0%)	60 (0%)	67 (12%)	71 (18%)	60 (0%)	60 (0%)	67 (12%)	75 (25%)
f10 m3/s)	0.03	0.0302 (1%)	0.0308 (3%)	0.0299 (0%)	0.0299 (0%)	0.0302 (1%)	0.0307 (2%)	0.0299 (0%)	0.0302 (1%)
f12 (m3/s)	0.01	0.0098 (2%)	0.0100 (0%)	0.0096 (4%)	0.0086 (14%)	0.0098 (2%)	0.0100 (0%)	0.0096 (4%)	0.0083 (17%)
f13 (m3/s)	0.01	0.0101 (1%)	0.0103 (3%)	0.0105 (5%)	0.0112 (12%)	0.0101 (1%)	0.0103 (3%)	0.0104 (4%)	0.0113 (13%)
f20 (m3/s)	0.03	0.0294 (2%)	0.0272 (9%)	0.0283 (6%)	0.0237 (21%)	0.0294 (2%)	0.0272 (9%)	0.0283 (6%)	0.0238 (21%)
f21 (m3/s)	0.01	0.0101 (1%)	0.0110 (10%)	0.0100 (0%)	0.0101 (1%)	0.0101 (1%)	0.0110 (10%)	0.0100 (0%)	0.0097 (3%)
f23 (m3/s)	0.01	0.0098 (2%)	0.0091 (9%)	0.0090 (10%)	0.0053 (47%)	0.0098 (2%)	0.0091 (9%)	0.0091 (9%)	0.0055 (45%)
f30 (m3/s)	0.03	0.0297 (1%)	0.0283 (6%)	0.0276 (8%)	0.0227 (24%)	0.0297 (1%)	0.0283 (6%)	0.0276 (8%)	0.0218 (27%)
f31 (m3/s)	0.01	0.0101 (1%)	0.0106 (6%)	0.0100 (0%)	0.0093 (7%)	0.0101 (1%)	0.0106 (6%)	0.0099 (1%)	0.0092 (8%)
f32 (m3/s)	0.01	0.0096 (4%)	0.0088 (12%)	0.0095 (5%)	0.0071 (29%)	0.0096 (4%)	0.0088 (12%)	0.0095 (5%)	0.0074 (26%)
C1 (mg/m3)	4.44	4.44 (0%)	4.4 (1%)	4.48 (1%)	4.56 (3%)	4.44 (0%)	4.41 (1%)	4.48 (1%)	4.55 (2%)
C2 (mg/m3)	1.11	1.11 (0%)	1.15 (4%)	1.15 (4%)	1.27 (14%)	1.11 (0%)	1.15 (4%)	1.15 (4%)	1.25 (13%)
C3 (mg/m3)	1.11	1.12 (1%)	1.17 (5%)	1.22 (10%)	1.48 (33%)	1.13 (2%)	1.17 (5%)	1.21 (9%)	1.52 (37%)

gradient of the parameter just evaluated has the steepest gradient now in the opposite direction. To eliminate this problem, the gradients of the objective function were evaluated at every iteration so that the search always followed the steepest path. While this increases the numerical computations conducted at each iteration, overshoot is also minimized, which in turn, decreases the number of iterations over which the model is evaluated. Hence, computational time is not significantly increased. No oscillations occurred and convergence was always achieved using this approach.

Tables 1, 2 and 3 summarize the estimated parameter values that result from the optimization, including the percent deviation from the actual value, and the steady-state concentrations from a unit release in Zone 1 for tracer gases released in each of the Zones, in Zones 1 and 2, and only in Zone 1, respectively. For comparison, Figs 4 and 5 illustrate the performance of the two algorithms in a scaled graphical format for the Case A and D measurements, respectively. Parameter estimates from Cases B and C are consistent with the results illustrated in Fig. 4, but, for brevity, are not illustrated here.

When sources are released in each of the zones (Table 1 and Figs 4 and 5), predicted parameter values in Cases A, B and C are in good agreement with the true values. Values predicted in Case D suggest less effective, though still reasonable estimates, given the limited quantity and quality of the synthetic measurements. Also, the predicted parameter values and the final value of the objective function from both algorithms are nearly identical for Cases A, B and C. This suggests that the solution field is well defined; and there are no significant local minimum combinations where the steepest descent algorithm becomes trapped. Differences in the predicted parameter values and the final value of the objective function for the Case D measurements, however, suggest that the combined infrequent and imprecise measurements cause considerable ill-definition of the system conditions.

To investigate the influence that the precision of the data had on the predictions, the combination of parameter values that yields the least sum of the squared error in the solution field (i.e., the 'best fitting' globally optimum combination) was found for Cases A and B using a full search of the parameter space.[3] The predicted values when gases were released in each zone for Cases A and B matched these combinations with less than one percent deviation. Hence, the global minimum combinations have been determined by the algorithms; the difference between the predicted and actual values is due to the imprecision of the data (i.e., if the data were precise (COV = 0), the global minimum combination would have been the actual values and the algorithms would have predicted them).

In cases with incomplete sets of measurements, where gases were released in only two or one of the three zones (Tables 2 and 3, respectively), estimates using the simulated annealing algorithm were generally better than those using the steepest descent algorithm for Cases A, B and C. This is due to the ill-definition of the solution field caused by insufficient concentration measurements to describe the flow characteristics in the zones where a gas was not released. In these cases, both algorithm

[3] Note that this method, which requires much more computational effort than either of the optimization techniques, would be unfeasible for applications with larger parameter spaces.

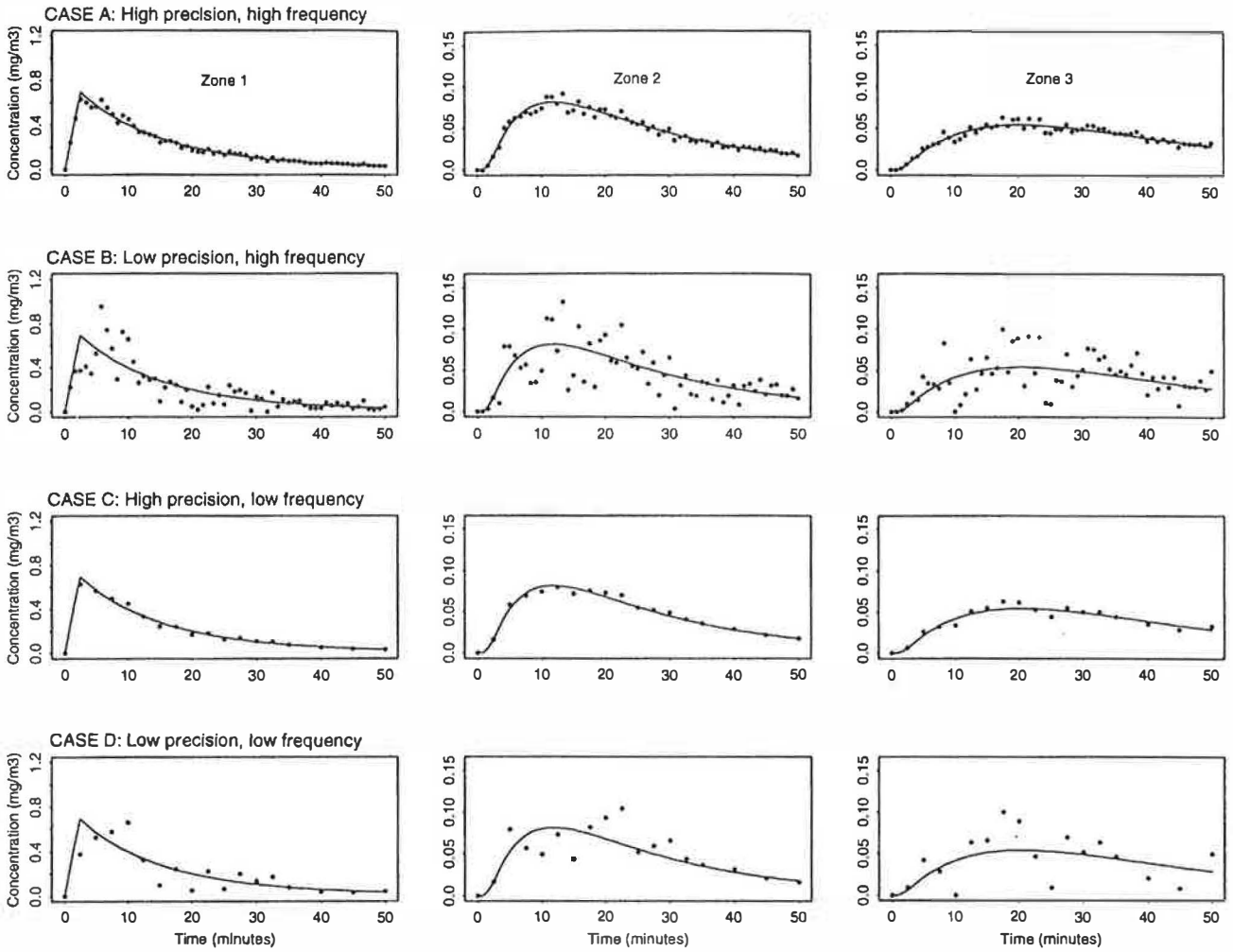

Fig. 3. Case-by-case illustration of the synthetic tracer gas measurements for a unit source release in Zone 1 for a duration of 150 s. The solid line is the simulated true concentrations; dots are the synthetic measurements obtained with normally distributed measurement error. High precision measurements are made with error having COV = 0.1; low precision measurements with error having COV = 0.5. High frequency measurements are made every 50 s. low frequency measurements are made every 150 s for the first 35 min and every 300 s thereafter. Similar synthetic tracer gas measurements are also simulated for a source release in Zone 2 and in Zone 3, but are not illustrated here for brevity.

concentrate their iterative parameter selections to match the better defined zones. This causes enough overshoot to alter the flow configuration such that flow to and from the zones that do not have tracer gas releases can no longer be accurately estimated. The steepest descent method falls into a local minimum parameter combination and is ineffective when this occurs. The simulated annealing algorithm, on the other hand, slowly settles down to its optimal combination so that even when the algorithm is at a local minimum, the mechanism for accepting poorer combinations allows it the opportunity to pass beyond the local minimum and continue with further parameter iterations. For the Case D measurements, however, the general breakdown of the optimization caused by the combined infrequent and imprecise measurements resulted in less consistent estimates for both methods.

Table 4 summarizes the final values of the objective function for each scenario. This value represents the fit of the predicted concentration profiles to the tracer gas measurements. When gases are released in each of the zones, the objective function is effectively identical. When fewer gases are released, the value estimated using the simulated annealing method is lower than that from the steepest descent method. This indicates that the computationally intensive method of simulated annealing has made better overall IAQ predictions. Furthermore, the predicted volumes and air exchange rates from the primary zones, (i.e., where a tracer gas was released: V_1, V_2, f_{10}, f_{12}, f_{20} and f_{21} in Table 2 and V_1 and f_{10} in Table 3) using the simulated annealing algorithm, deviate by less than 35 and 45% from their actual values, respectively. This suggests that approximate parameter estimates for zones which are of particular interest in a flow investigation can be made, even when a complete tracer gas release experiment cannot be conducted.

Table 2
Summary of the optimization results for the condition when a different tracer gas was released in Zones 1 and 2. The percent error from the actual values are in parentheses. C1, C2 and C3 are the steady-state concentration for a unit release in Zone 1 for Zones 1, 2 and 3 respectively

		Steepest descent				Simulated annealing			
Case:	Actual	A	B	C	D	A	B	C	D
V1 (m3)	40	41 (3%)	45 (13%)	42 (5%)	50 (25%)	41 (3%)	44 (10%)	42 (5%)	49 (23%)
V2 (m3)	20	18 (10%)	13 (35%)	18 (10%)	13 (35%)	18 (10%)	13 (35%)	18 (10%)	13 (35%)
V3 (m3)	60	4 (93%)	5 (92%)	4 (93%)	6 (90%)	41 (32%)	41 (32%)	34 (43%)	35 (42%)
f10 (m3/s)	0.03	0.0375 (25%)	0.0381 (27%)	0.0376 (25%)	0.0384 (28%)	0.0338 (13%)	0.0363 (21%)	0.0341 (14%)	0.0341 (14%)
f12 (m3/s)	0.01	0.0107 (7%)	0.0107 (7%)	0.0103 (3%)	0.0088 (12%)	0.0089 (11%)	0.0048 (52%)	0.0090 (10%)	0.0069 (31%)
f13 (m3/s)	0.01	0.0007 (93%)	0.0010 (90%)	0.0007 (93%)	0.0014 (86%)	0.0069 (31%)	0.0083 (17%)	0.0059 (41%)	0.0076 (24%)
f20 (m3/s)	0.03	0.0368 (23%)	0.0340 (13%)	0.0354 (18%)	0.0277 (8%)	0.0326 (9%)	0.0298 (1%)	0.0321 (7%)	0.0255 (15%)
f21 (m3/s)	0.01	0.0113 (13%)	0.0122 (22%)	0.0110 (10%)	0.0108 (8%)	0.0104 (4%)	0.0105 (5%)	0.0106 (6%)	0.0104 (4%)
f23 (m3/s)	0.01	0.0006 (94%)	0.0007 (93%)	0.0006 (94%)	0.0005 (95%)	0.0068 (32%)	0.0114 (14%)	0.0050 (50%)	0.0036 (64%)
f30 (m3/s)	0.03	0.0000 (100%)	0.0000 (100%)	0.0000 (100%)	0.0000 (100%)	0.0117 (61%)	0.0075 (75%)	0.0115 (62%)	0.0135 (55%)
f31 (m3/s)	0.01	0.0000 (100%)	0.0000 (100%)	0.0000 (100%)	0.0000 (100%)	0.0059 (41%)	0.0000 (100%)	0.0025 (75%)	0.0000 (100%
f32 (m3/s)	0.01	0.0032 (68%)	0.0043 (57%)	0.0031 (69%)	0.0055 (45%)	0.0172 (72%)	0.0545 (445%)	0.0138 (38%)	0.0173 (73%)
C1 (mg/m3)	4.44	4.34 (2%)	4.28 (4%)	4.34 (2%)	4.38 (1%)	4.4 (1%)	4.31 (3%)	4.39 (1%)	4.39 (1%)
C2 (mg/m3)	1.11	1.02 (8%)	1.08 (3%)	1.03 (7%)	1.16 (5%)	1.17 (5%)	1.26 (14%)	1.16 (5%)	1.31 (18%)
C3 (mg/m3)	1.11	1.11 (0%)	1.15 (4%)	1.12 (1%)	1.21 (9%)	1.11 (0%)	0.81 (27%)	1.14 (3%)	1.23 (11%)

Table 3
Summary of the optimization results for the condition when a different tracer gas was released in Zone 1. The percent error from the actual values are in parentheses. C1, C2 and C3 are the steady-state concentrations for a unit release in Zone 1 for Zones 1, 2 and 3, respectively

		Steepest descent				Simulated annealing			
Method: Case:	Actual	A	B	C	D	A	B	C	D
V1 (m3)	40	41 (3%)	44 (10%)	42 (5%)	50 (25%)	41 (3%)	44 (10%)	42 (5%)	50 (25%)
V2 (m3)	20	1 (95%)	1 (95%)	1 (95%)	1 (95%)	5 (75%)	5 (75%)	5 (75%)	3 (85%)
V3 (m3)	60	2 (97%)	1 (98%)	2 (97%)	2 (97%)	29 (52%)	26 (57%)	28 (53%)	22 (63%)
f10 (m3/s)	0.03	0.0461 (54%)	0.0469 (56%)	0.0460 (53%)	0.0454 (51%)	0.0401 (34%)	0.0400 (33%)	0.0389 (30%)	0.0384 (28%)
f12 (m3/s)	0.01	0.0004 (96%)	0.0005 (95%)	0.0004 (96%)	0.0004 (96%)	0.0025 (75%)	0.0026 (74%)	0.0026 (74%)	0.0027 (73%)
f13 (m3/s)	0.01	0.0003 (97%)	0.0001 (99%)	0.0003 (97%)	0.0005 (95%)	0.0051 (49%)	0.0049 (51%)	0.0054 (46%)	0.0052 (48%)
f20 (m3/s)	0.03	0.0016 (95%)	0.0018 (94%)	0.0015 (95%)	0.0013 (96%)	0.0113 (62%)	0.0117 (61%)	0.0132 (56%)	0.0141 (53%)
f21 (m3/s)	0.01	0.0002 (98%)	0.0000 (100%)	0.0002 (98%)	0.0001 (99%)	0.0000 (100%)	0.0000 (100%)	0.0000 (100%)	0.0000 (100%
f23 (m3/s)	0.01	0.0002 (98%)	0.0003 (97%)	0.0002 (98%)	0.0002 (98%)	0.0018 (82%)	0.0018 (82%)	0.0006 (94%)	0.0157 (57%)
f30 (m3/s)	0.03	0.0009 (97%)	0.0004 (99%)	0.0011 (96%)	0.0021 (93%)	0.0115 (62%)	0.0157 (48%)	0.0167 (44%)	0.0153 (49%)
f31 (m3/s)	0.01	0.0002 (98%)	0.0002 (98%)	0.0002 (98%)	0.0000 (100%)	0.0064 (36%)	0.0000 (100%)	0.0006 (94%)	0.0000 (100%
f32 (m3/s)	0.01	0.0002 (98%)	0.0002 (98%)	0.0002 (98%)	0.0000 (100%)	0.0030 (70%)	0.0027 (73%)	0.0042 (58%)	0.0237 (137%
C1 (mg/m3)	4.44	4.28 (4%)	4.22 (5%)	4.29 (3%)	4.32 (3%)	4.35 (2%)	4.21 (5%)	4.29 (3%)	4.32 (3%)
C2 (mg/m3)	1.11	1.05 (5%)	1.01 (9%)	1.08 (3%)	1.18 (6%)	1.1 (1%)	1.05 (5%)	1.13 (2%)	1.25 (13%)
C3 (mg/m3)	1.11	1.16 (5%)	1.2 (8%)	1.12 (1%)	1.1 (1%)	1.15 (4%)	1.21 (9%)	1.1 (1%)	1.08 (3%)

Predicted steady-state concentrations resulting from a unit release in Zone 1 were determined for each scenario and compared to the 'true' steady-state concentrations, as a method of investigating the effects of the errors in the parameter estimation. Predicted concentrations show good agreement with the true concentrations for all cases and tracer gas release scenarios. This suggests that for long-term IAQ assessments, where exact flow characterization may not be essential for the assessment, these methods may still be appropriate for quantifying some of the concentration gradients in large, heterogeneous, partitionless buildings, even if considerable uncertainty is present in the selection of appropriate surrogate zone volumes and their exchange flows.

The demonstration and results presented here are for selected cases and conditions that are thought to span typical building systems. However, under different site conditions where compartment volumes and air exchange rates may differ by orders of magnitude, the IAQ model may not be appropriate due to ill-conditioned systems of equations. Under such cases a more appropriate IAQ model must first be designed and appropriate

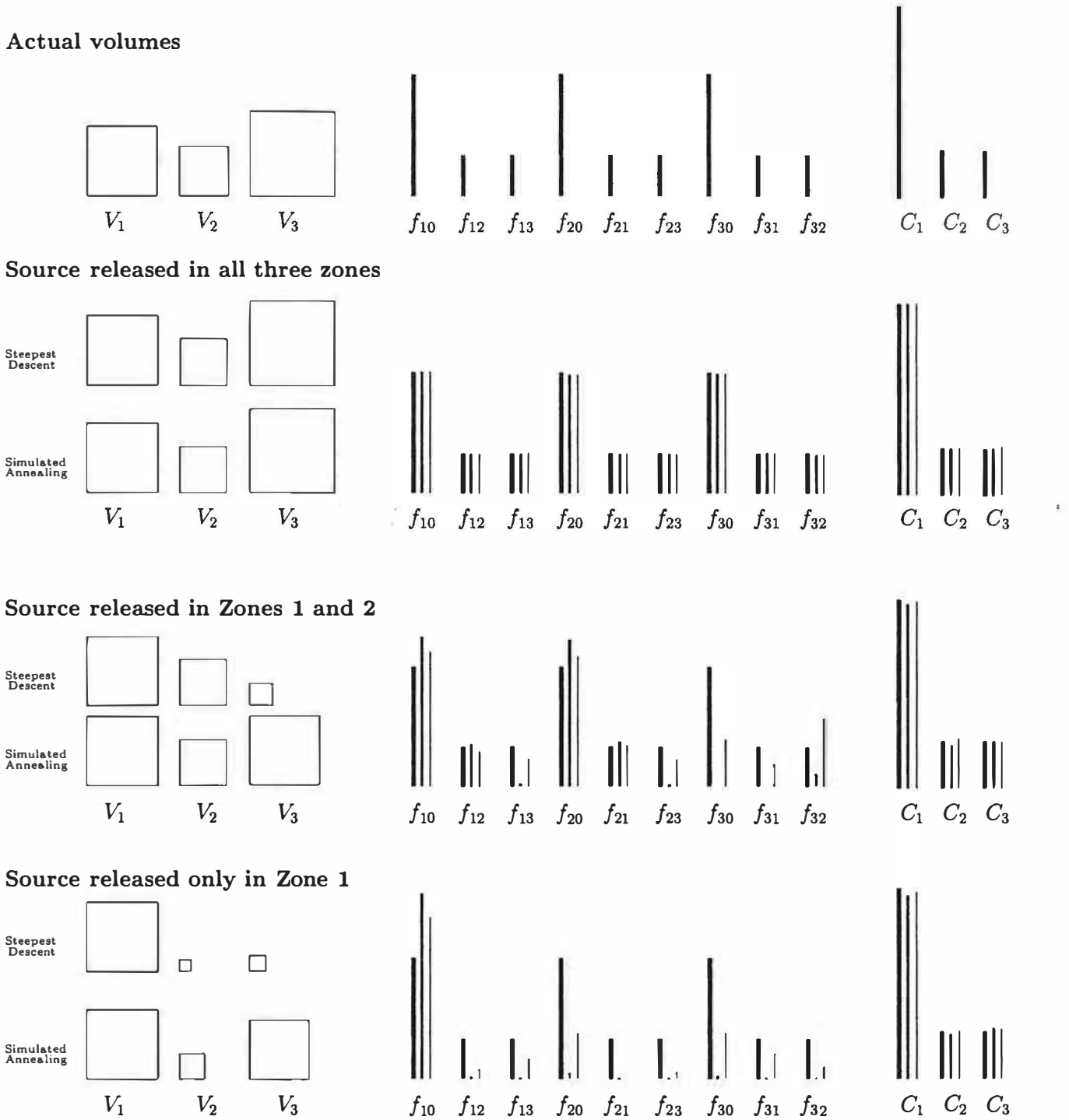

Fig. 4. Illustration of the steepest descent and simulated annealing parameter optimization for Case A measurements. The area depicted by the volume represents the floor area (i.e., 'footprint') of a one-meter tall zone. The air exchange rates and steady-state concentrations for a unit release in Zone 1 are summarized with the thickest line representing the actual value (▮), followed by the steepest descent (▌) and simulated annealing (▏) predictions, respectively.

optimization schemes investigated further. Nevertheless, for those cases, it is likely that optimization techniques will be the only available general method of calibration since analytical methods are unlikely to be applicable over the full range of possible conditions.

4. Summary and concluding remarks

The steepest descent and simulated annealing optimization techniques were used to simultaneously estimate the effective mixing volumes and air exchange rates of a

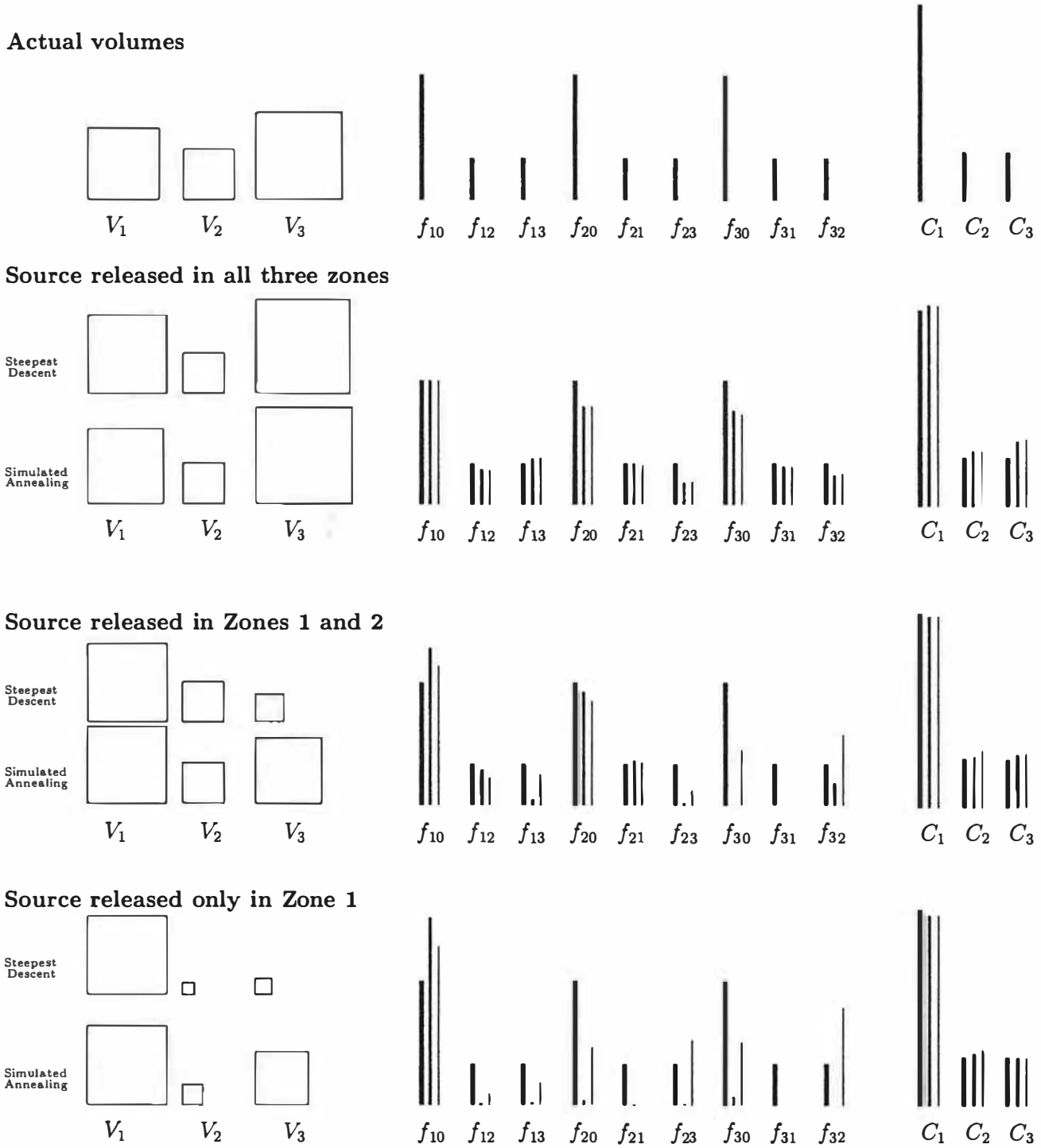

Fig. 5. Illustration of the steepest descent and simulated annealing parameter optimization for Case D measurements. The area depicted by the volume represents the floor area (i.e., 'footprint') of a one-meter tall zone. The air exchange rates and steady-state concentrations for a unit release in Zone 1 are summarized with the thickest line representing the actual value (▮), followed by the steepest descent (▌) and simulated annealing (▏) predictions, respectively.

three-zone model for three levels of available data: (i) tracer gases releases in all three zones; (ii) in Zones 1 and 2; and (iii) only in Zone 1; and for four measurement conditions ranging from precise (COV = 0.1) and frequent (every 50 s), to imprecise (COV = 0.5) and infrequent (every 150 s for 35 min and every 300 s thereafter). The motivation for the analysis is to develop a method for making IAQ predictions in a large building exhibiting heterogeneous spatial air flow conditions by representing it as a combination of several well-mixed

Table 4
Summary of the values of the objective function (i.e., the sum of the squared error between predicted and measured concentrations) at parameter estimation completion for each measurement case and release scenario

	Tracer gas released in each zone		Tracer gas released in Zones 1 & 2		Tracer gas released in Zone 1	
Case	Steepest descent	Simulated annealing	Steepest descent	Simulated annealing	Steepest descent	Simulated annealing
A	0.1954	0.1954	0.1555	0.1474	0.0355	0.0346
B	4.7643	4.7643	3.6312	3.5271	0.8920	0.8910
C	0.0267	0.0267	0.0149	0.0137	0.0091	0.0088
D	0.7313	0.7235	0.3461	0.3440	0.2376	0.2370

partitionless surrogate zones. However, there is no analytical transformation that can be used to either simultaneously estimate volumes and air exchange rates, or to consider cases where tracer gases are not released in each of the surrogate zones.

Constraints on the optimization routines were limited to non-negative parameters and a maximum total volume constraint. When tracer gases are released in all three zones, the solution field is well-defined so that there are no significant local minimum combinations, and the more efficient steepest descent algorithm can be used. In cases of incomplete sets of measurements, local minimum combinations can prevent the steepest descent algorithm from finding the global minimum. The simulated annealing algorithm yielded improved estimates for those zones in which a tracer gas was released and a better overall fit to the tracer gas measurements.

Steady-state concentrations for a unit source release in Zone 1 exhibited good agreement with the actual simulated concentrations for all cases and tracer gas release scenarios. This suggests the use of surrogate zones, with appropriate optimization methods for parameter estimation, can offer a reasonable approach for estimating IAQ in long-term assessments in large, heterogeneous, partitionless buildings.

Acknowledgements

This research was funded in part by the University of Pittsburgh under subcontract agreement number 7197-2, and The Concurrent Technologies Corporation under subcontract agreement number 930500072 in support of U.S. Department of Defense contract number DAAA21-0046. The research benefited from input and discussion with Dr Urmila Diwekar and Dr James Axley.

References

[1] I'Anson S, Irwin C, Howarth A. Air flow measurement using three tracer gases. Building and Environment 1982;17(4):245–52.
[2] Sandberg M. What is ventilation efficiency? Building and Environment 1981;16(2):123–35.
[3] Sinden FW. Multi-chamber theory of air infiltration. Building and Environment 1978;13:21–68.
[4] Lagus P, Persily A. A review of tracer-gas techniques for measuring airflows in buildings. ASHRAE Transactions 1985;91:1075–87.
[5] Sherman M. Tracer-gas techniques for measuring ventilation in a single zone. Building and Environment 1990;25(4):365–74.
[6] Sandberg M, Stymne H. The constant tracer flow technique. Building and Environment 1989;24(3):209–19.
[7] Axley JW. Multi-zone dispersal analysis by element assembly. Building and Environment 1989;24(2):113–30.
[8] O'Neill P, Crawford R. Identification of flow and volume parameters in multizone systems using a single-gas tracer technique. ASHRAE Transactions 1991;97:49–54.
[9] Bard Y. Nonlinear Parameter Estimation. Academic Press, 1974.
[10] Diwekar UM, Pitchumani P. Optimal cure cycles for thermoset composites manufactures. In: HTD-Vol. 241, Advanced Computations in Material Processing, Prasad V, Arinilli R, editors. The American Society of Mechanical Engineers, 1993, pp. 23–31.
[11] Seinfeld JH, Lapidus L. Mathematical Methods in Chemical Engineering: Volume 3, Process Modeling, Estimation, and Identification. Prentice-Hall, Inc., 1966.
[12] Rutenbar RA. Simulated annealing algorithms: An overview. IEEE Circuits and Devices, 1989, pp. 19–26.
[13] Kirkpatrick S, Gelatt JCD, Vechi, M. Optimization by simulated annealing. Science 1983;220(4598):671–80.
[14] Press WH, Teukolsky SA, Vetterling WT, Flannery BP. Numerical Recipes in FORTRAN: The Art of Scientific Computing, 2nd edn. Cambridge University Press, 1992.
[15] Boyce WE, DiPrima RC. Elementary Differential Equations and Boundary Value Problems, 4th edn. John Wiley & Sons, 1986.